JOURNAL OF MACROMOLECULAR SCIENCE®
Part B—Physics
Vol. B43, No. 1, pp. 59–70, 2004

Lamellar Ordering and Crystallization in a Symmetric Block Copolymer[#]

Liangbin Li, Denitza Lambreva, and Wim H. de Jeu*

FOM-Institute for Atomic and Molecular Physics,
Amsterdam, The Netherlands

ABSTRACT

By using time-resolved small-angle x-ray scattering, the crystallization and melting behavior in an ordered lamellar morphology has been investigated for a symmetric short-chain poly(ethylene oxide)-*b*-butadiene (PEO-*b*-PB_h) block copolymer. The long period of the crystallized lamella continuously increases with the crystallization temperature, and no integer number of stems can be assigned to the folded chain crystals. The effects of deviations of the poly(ethylene oxide) (PEO) and PB chains from a Gaussian coil in the ordered phase on the PEO crystallization are evaluated and modeled. Samples cooled fast from different temperatures in the molten state reveal a significant coupling between lamellar ordering and crystallization. The reorganization of the chains during cooling promotes nucleation and shortens the induction period.

Key Words: Crystallization; Lamellar ordering; PEO-*b*-PB_h; Avrami index.

*Correspondence: Wim H. de Jeu, FOM-Institute for Atomic and Molecular Physics, Kruislaan 407, 1098 SJ, Amsterdam, The Netherlands; E-mail: dejeu@amolf.nl.

[#]Presented at the conference 'Synchrotron Radiation in Polymer Science II', Sheffield, UK, 4–6 September 2002.

DOI: 10.1081/MB-120027751 0022-2348 (Print); 1525-609X (Online)

INTRODUCTION

The coupling of different phase transitions in polymer systems can create a rich variety of structures and morphologies with potential applications in optics and microelectronics.[1,2] Examples are the coupling between (liquid-)crystalline ordering and block copolymer organization.[3–13] The inherent complexity of amorphous block copolymers that self-organize into lamellar, cylindrical, or other microphase-separated structures because of incompatible blocks[14–16] is greatly increased when one of the blocks is semicrystalline.[4,7–13,17–20] Crystallization within a microphase-separated structure can lead to improved mechanical, optical, and other properties. Because the length scales of microphase-separated block copolymers are in the range of 10–50 nm, new types of semicrystalline nanocomposite material are possible that cannot be achieved with homopolymers.

The crystallization behavior of crystalline/amorphous block copolymers also is interesting because of the potential to give new insights into polymer crystallization.[16] Theoretically, competition between the preferred conformation of each of the blocks, i.e., unfolded chains for the crystallized component and randomly coiled chains for the amorphous one, results in an equilibrium degree of chain folding in the crystalline layers.[10–21] However, experimentally, it is difficult to obtain thermodynamically stable folded chain crystals in block copolymer systems. Recently, a continuous variation of the lamellar spacing with the crystallization temperature has been reported for poly-(ethylene oxide)-*b*-butadiene (PEO-*b*-PB_h).[22] In a block copolymer, crystallization can take place in a phase-separated morphology. The resulting confinement has a strong influence on the crystallization of crystallizable block, especially when the size of the ordered domains is smaller than that of the crystallized ones. Depending on the order–disorder transition temperature T_{ODT}, the crystallization temperature T_{cr} of the crystallizable block, and the glass transition temperature of amorphous block T_g, the confinement can be hard ($T_{cr} < T_g < T_{ODT}$) or soft ($T_g < T_{cr} < T_{ODT}$). The type of morphology (lamellae, cylinders, or spheres) determines whether the confinement is one-, two-, or three-dimensional, respectively.[4,9,12] However, because of the covalent connection between the amorphous and the crystalline block, the confinement is not simply geometrical. Both theory and experiment indicate that the molecular chains are highly stretched in the ordered phase well below T_{ODT}, creating a low-entropy molten state.[3,15] This can be expected to influence the nucleation process and thus the crystallization kinetics. Furthermore, the crystallization and the ordering process may interact and couple. Numerical simulations show that nucleation can be significantly enhanced by critical density fluctuations.[23] Hence, we anticipate, in a supercooled block copolymer melt, that density fluctuations during reorganization of the chains promote nucleation.

In this article, we describe the crystallization of PEO in a symmetric PEO-*b*-PB_h block copolymer, which is investigated by small-angle x-ray scattering (SAXS). The confinement is soft, as T_{cr} is lower than T_{ODT} ($>300^\circ C$) but higher than T_g ($<-50^\circ C$). We describe the effect on the PEO crystallization of the strain due to the microphase separation, as well as the dynamic coupling between the ordering of the molecular chains and the crystallization. Both the strain and the density fluctuations during reorganization promote nucleation and shorten the induction period.

EXPERIMENTAL

Low molecular weight diblock copolymers PEO-*b*-PB_h were obtained from Th. Goldschmidt (Essen, Germany). They were produced by hydrogenation of the polybutadiene block, leading to about 50% 1–2 and 50% 1–4 units, statistically distributed. The block sizes were 4.3 kg/mol for PEO and 3.7 kg/mol for PB_h with a polydispersity of 1.08. The volume fractions of the PEO block before and after crystallization were about 47% and 44.5%, respectively. The length of a nonfolded crystalline PEO block is 27.3 nm.

In situ SAXS measurements were done with an in-house setup consisting of a rotating anode x-ray generator (Rigaku RU-300H, 18 kW, focus $0.5 \times 1\,mm^2$), equipped with two parabolic multilayer mirrors (Bruker, Karlsruhe). This lead to a monochromatized CuK_α beam (wavelength $\lambda = 0.154$ nm) that was highly parallel (divergence about 0.012°). In this situation, the x-ray flux was about an order of magnitude larger compared with conventional slit-pinhole collimation and a nickel filter. The beam size was defined by two sets of slit-pinholes. In addition, a guard slit-pinhole was placed in front of the sample to cut parasitic scattering from the beam-defining slits and the mirrors. The SAXS intensity was collected by a two-dimensional gas-filled wire detector (Bruker Hi-star). A semitransparent beamstop was placed in front of the area detector, which allowed monitoring of the beam intensity.

A Linkam CSS450 temperature-controlled shear system was used as sample stage. Samples were kept in a brass sample holder with kapton windows replacing the glass windows of the original system. Large cooling rates were achieved by applying a liquid nitrogen flow. Samples were first heated up to 100°C for 10 min, and then cooled down with a cooling rate of 30°C/min to the predetermined temperature for isothermal crystallization. The SAXS measurements at 30 s/frame were started immediately when the set temperature was reached. After completion of the crystallization—as indicated by the saturated SAXS intensity—the samples were heated at a slow rate of 0.5°C/min. This melting process also was monitored *in situ* by SAXS.

RESULTS

Figure 1(a) shows a typical integrated one-dimensional SAXS profile of PEO-*b*-PB_h during crystallization at 48°C. The *x* axis represents the modulus of the scattering vector q, with $q = (4\pi/\lambda)/\sin\theta$, where θ is the scattering angle. The *y* axis displays the Lorentz-corrected scattering intensity from the randomly oriented lamellar structure multiplied by q^2 (the so-called invariant). The crystallization takes place in the lamellar phase as indicated by the peak at $q \approx 0.32\,nm^{-1}$. The peak at smaller values ($q \approx 0.25\,nm^{-1}$) appears only after about 5 mm and corresponds to crystallized lamellae. As T_{cr} of the PEO block is much larger than T_g of the PB_h-block, the confinement is soft. A Gaussian fitting of the first-order peak leads to the crystalline lamellar spacing and normalized scattered intensity presented in Fig. lb. We note a strong thickening of the crystallized lamellae during the crystallization process. The crystallization kinetics can be described by the Avrami equation:

$$X_{cr} = 1 - \exp(-KT_{cr}{}^n) \tag{1}$$

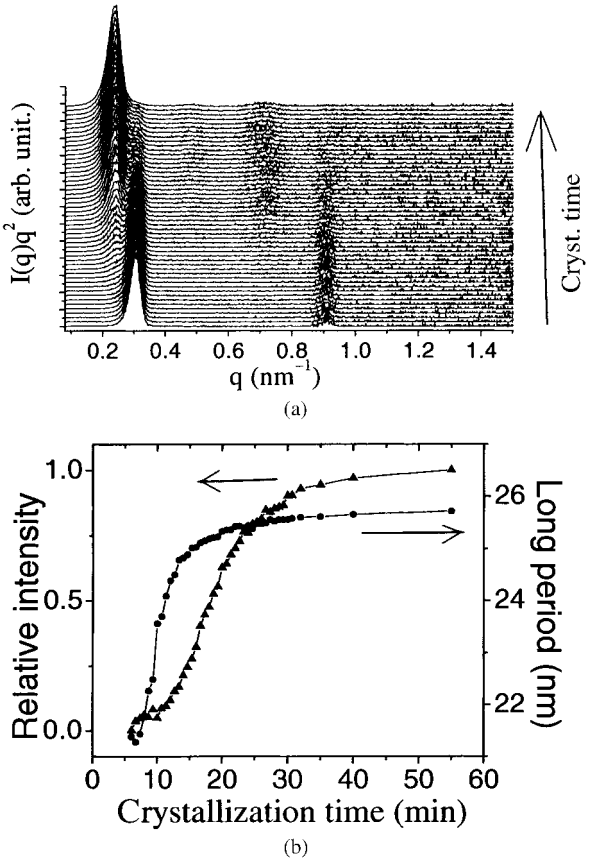

Figure 1. Isothermal crystallization of PEO-*b*-PB_h at 48°C. (a) SAXS measurements. (b) Long period and normalized scattering intensity of the first-order peak from the crystallized lamellae.

where X_{cr} is the crystalline fraction, and K and n are the Avrami constant and index, respectively, plotted in Fig. 2. The Avrami index has values around 3.0 or even somewhat larger, similar as found for homopolymers.

Figure 3 shows the long period associated with the lamellae before and after crystallization as a function of temperature. The long period of the crystallized lamellae reflects samples isothermally crystallized at that temperature. Above T_{cr}, the lamellar spacing increases approximately linearly with decreasing temperature. This can be attributed to an increase of the Flory-Huggins parameter χ, which varies as $1/T$. Consequently, the microphase separation becomes stronger and the interface thickness decreases when the temperature is lowered. On the other hand, the crystallized lamellar spacing is larger for a high crystallization temperature. Between 40°C to 53°C, the long period of the crystallized lamellae varies approximately linearly with temperature and, hence, with the amount of supercooling ΔT. This can be contrasted with stepwise changes in a corresponding block copolymer film,[24] as well as in a similar low-molecular weight PEO homopolymer.[25] By taking the volume fraction of the PEO and the PB_h blocks into

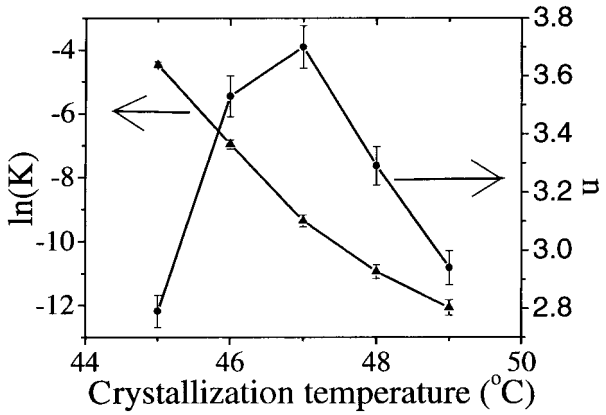

Figure 2. Variation of the Avrami parameters K and n with crystallization temperature.

account and assuming the molecular chains to be perpendicular to the lamellae, we calculate that the PEO crystals consist of noninteger-folded chains.

For the present PEO-*b*-PB_h block copolymer, T_{ODT} could not be reached, even for temperatures up to 300°C. The large difference between T_{ODT} and T_{cr} prevents any direct coupling between the ordering transition and crystallization. However, as shown in Fig. 3, the lamellar spacing before crystallization increases with decreasing temperature, indicating a reorganization of the molecular chains. Hence, a jump to a specific crystallization temperature from a different temperature in the amorphous melt will introduce a different melt memory. The associated difference in the chain-ordering process could change the crystallization behavior. To test this point, two samples were investigated, both kept initially for 30 min at 150°C. Sample I was directly cooled down to crystallize at 48°C, while sample II was first cooled down to 60°C, kept for 30 min to equilibrate, and then also crystallized at 48°C. The SAXS measurements following the crystallization are shown in Figs. 4a and b, the relative scattered intensity vs.

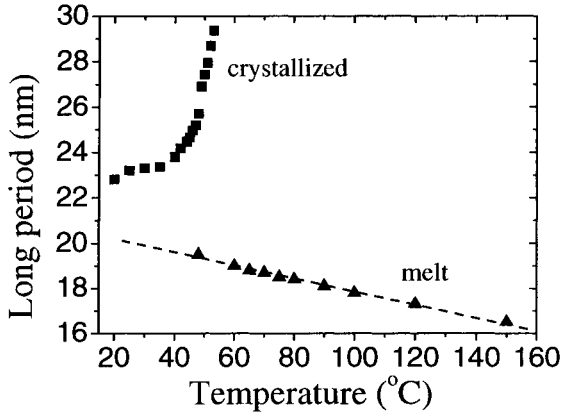

Figure 3. Long period of the PEO-*b*-PB_h lamellae, crystallized, and in the melt.

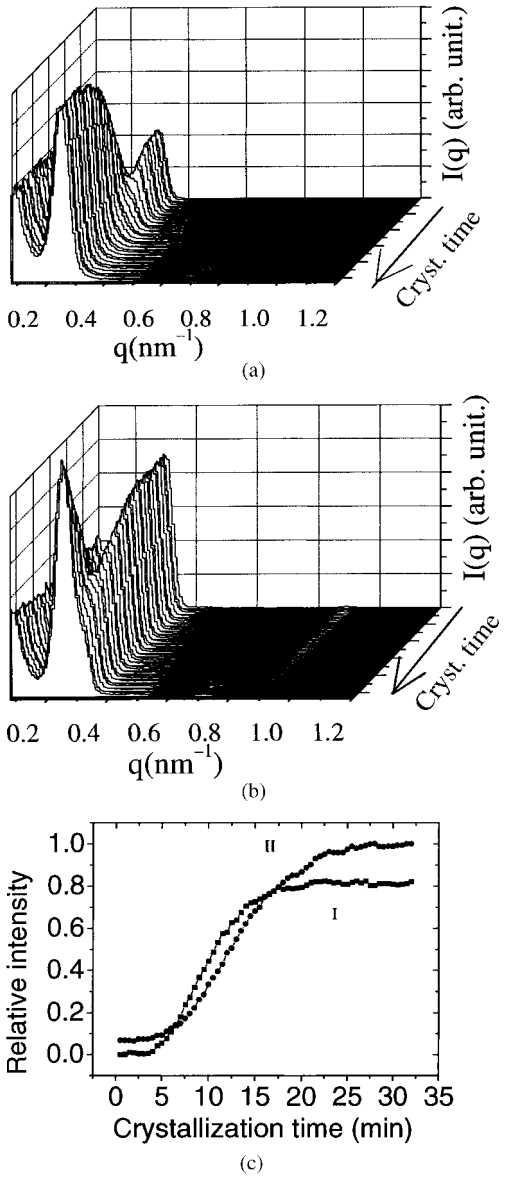

Figure 4. Small-angle x-ray scattering patterns of PEO-*b*-PB_h crystallized at 48°C. (a) Quenched from 150°C (I). (b) Quenched from 60°C (II). (c) Comparison of the normalized scattering intensity of samples I and II, respectively, which both contain scattering from the melt, as well as from the crystallized lamellae.

crystallization time is indicated in Fig. 4c. Compared with sample II, sample I nucleates faster with a shorter induction time, but it has a lower final crystallinity.

Once the crystallization at a specific temperature was completed, SAXS measurements were taken during slow heating. Figure 5 shows the normalized scattering

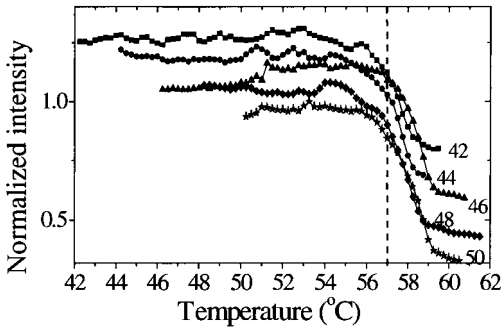

Figure 5. Normalized scattering intensity of PEO-*b*-PB_h, crystallized at the temperatures indicated, during slow heating at 0.5°C/min. Curves have been shifted for clarity.

intensity vs. temperature. During the heating process, some small peak shifts (~0.5 nm) were observed for samples crystallized below 45°C, not for samples crystallized at higher temperatures. Hence, no thickening occurs during the heating process. Although the samples crystallized at different temperature have different lamellar thicknessess, the melting points are approximately the same (around 57°C). Oscillations of the scattered intensity suggest a reorganization of the lamellae during heating.

DISCUSSION

A crucial picture in relation to the crystallization process is Fig. 1b. which shows that the lamellar thickening is faster than the increase of the scattered intensity. The long period of crystallized lamella reaches its plateau value after about 12 min, while this takes, for the scattered intensity, 30 min. If the thickening process would take place along the full block interfaces, one would expect both processes to develop in parallel. The experimental results can be explained if the PEO crystals grow laterally as schematically shown in Fig. 6, which is similar to the thickening process of polyethylene crystallized at high pressure.[26] A transition region of length L_{tr} is introduced to avoid a sharp edge at the boundary between noncrystallized and crystallized lamella. The length L_{tr} is small and

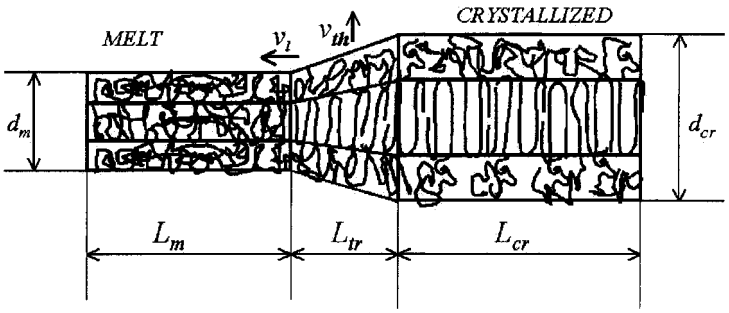

Figure 6. Schematic picture of the thickening model of confined crystallization in a lamellar block copolymer.

should not change with the crystallization time. Hence, relative to the crystallized lamellae, the importance of L_{tr} in determining the lamellar period decreases rapidly. On the other hand, the crystallinity is mainly determined by the ratio between crystallized and noncrystallized lamellae, which takes much more time to grow. Hence, this model can explain the difference between the rate of thickening and the overall growth rate. In this picture, the crystal growth front keeps a wedge shape, while growing simultaneously in both the lateral direction (ν_l) and along the chain axis (thickening ν_{th}).

Let us consider the crystallization process in more detail. First, the crystal growth rate G of a homopolymer melt can be expressed as:[27,28]

$$G_h = G_0 \exp\left(-\frac{\Delta E}{RT}\right) \exp\left(-\frac{\Delta F}{RT}\right) \tag{2}$$

where G_0 is a constant, ΔE the activation energy for migration through a nucleus–melt interface, ΔF the free energy for formation of a nucleus of critical size, T the crystallization temperature, and R the gas constant. To generalize this expression to an ordered block copolymer melt, three terms should be added. The first one is the activation energy ΔE_{am} for the displacement forced upon the amorphous block by the crystalline block during crystallization. The second one is the entropy $-\Delta F_{cr}$ associated with the prestretching of the crystallizable block built-in already in the ordered state. Finally, if the size of the critical nucleus is larger than the lamellar spacing in the melt, the amorphous block loses another amount of entropy ΔF_{am} during the nucleation process: the formation of a critical nucleus requires a larger spacing and thus stretches amorphous block even further. Hence, the crystal growth rate in a block copolymer can be written as

$$G_{co} = G_0 \exp\left(-\frac{\Delta E + \Delta E_{am}}{RT}\right) \exp\left(-\frac{\Delta F - \Delta F_{cr} + \Delta F_{am}}{RT}\right) \tag{3}$$

Though this extended equation should not be considered fully quantitatively, it can serve nicely to illustrate the various contributions. The factor ΔE_{am} contains the effect of geometrical confinement on the diffusion process, which will slow down the crystallization process. The geometrical confinement on the nucleation is included in ΔF_{am}. If the critical size of the nucleus is smaller than the lamellar spacing in the melt, $\Delta F_{am} = 0$, and nucleation in an ordered block copolymer can be faster than that in the corresponding homopolymer because of the prestretching given by $-\Delta F_{cr}$. Even if ΔF_{am} is nonzero but smaller than ΔF_{cr}, this is still the case. When nucleation needs a larger space, as found for small supercooling, ΔF_{am} overcompensates $-\Delta F_{cr}$ and the PEO block disturbs amorphous block during nucleation. This indicates that geometrical confinement is stronger at small supercooling than at large supercooling, because it slows down both nucleation and diffusion. At large supercooling, the increased nucleation in the block copolymer may be compensated by the decreased diffusion leading to an overall crystallization behavior similar to the homopolymer. These effects are nicely reflected in the Avrami index, that shows a local maximum around 47°C.

When a sample is cooled down from a high temperature to a temperature below the melting point, two processes occur: ordering (or reorganization) and crystallization, schematically shown in Fig. 6. The results of Fig. 4 indicate a coupling between these two effects. When a sample is cooled down, the lamellar spacing increases. During this process of moving to a new stretched equilibrium position, each chain develops a certain

velocity. These local movements, in turn, will promote nucleation. The larger velocities associated with the larger temperature jump of sample I compared with II thus cause a shorter induction time. After equilibrating at 60°C, the interface between the PEO and the PB_h blocks is for sample II narrower than in sample I cooled from 150°C. This is reflected in the larger scattering intensity (10%) of sample II at the onset of crystallization. In addition, the PEO segments can crystallize more perfectly at the sharp interfaces, leading to a 20% larger final scattering intensity (higher crystallinity) than for sample I. As has been discussed elsewhere,[29] this type of coupling becomes more complicated if T_{cr} and T_{ODT} are close, in which situation both thermodynamic and kinetic effects come into play.

The long period of the crystallized PEO lamellae increases continuously with the crystallization teniperature (Fig. 3). Hence integer-folded chain crystals cannot be assigned to the structures. This can be contrasted to low-molecular mass PEO homopolymers for which noninteger-folded chain crystals are metastable and only observed at the beginning of the crystallization.[30] For homopolymers, thickening through sliding diffusion is easy, especially during slow heating.[31] This is different in our bulk block copolymer system because of the attached amorphous block. We suppose that the crystals with $L = 29.4$ nm obtained at 53°C are equilibrium-folded chain crystals with approximately one fold. According to the volume fraction PEO, this would correspond to a crystal thickness of $0.445 \times 29.4 = 13.1$ nm. Twice this value is in reasonable agreement with the extended chain length of 27.3 nm. Other crystals grown at lower temperatures are nonequilibrium crystals.

The relative stability of noninteger-folded chain crystals in bulk block copolymer systems can be attributed to two reasons. First, due to the loss of entropy due to attendant stretching of the amorphous block, the Gibbs free-energy landscape between integer-folded chain crystals $(n, n + 1)$ will be rather flat. This reduces the thermodynamic driving force toward integer-folded chains in comparison with homopolymers. Second, kinetically, the thickening process must overcome not only the internal friction within the PEO crystals but also that within the amorphous part.[32,33] However, in thin, uniformly oriented films of the same PEO-*b*-PB_h system, integer-folded crystals were observed.[24] We tentatively attribute the difference with the bulk situation to the two-dimensional crystallization process in thin films, which causes the lateral sliding again to be important, as in PEO homopolymers.

The above arguments also can explain why the crystals with different thickness still have about the same melting point. The thickness of lamellar crystals of the PEO block is compatible with a range between one and two folds (Fig. 3). Hence, an increase of the lamellar thickness with crystallization temperature does not change the number of folds, and the theoretical calculations for a change in folding in block copolymers by DiMarzio et al.[19] and by Whitmore and Noolandi[20] do not apply. In our block copolymer system, the crystals gain surface free energy by thickening. Otherwise one would not expect a lower free energy for thicker crystals, as thickening gives less favorable statistical conformations of the amorphous molecular chains. The compromise between thick crystals and favorable statistical conformations of the amorphous block makes the free energy landscape very flat, especially for the region close to equilibrium. This results in a weak dependence of the melting temperature on the lamellar thickness.

We want to finish with two general remarks about the crystallization behavior of polymers, in general, in connection with what we can learn from crystallizable block

copolymers. The first one regards the memory of a polymer melt or its thermal history, the subject of which is under considerable debate. In ordered block copolymers, one can put the crystallizable chains in a specific stretched state by choosing an appropriate temperature. The loss of entropy can be evaluated from the balance between the interface free energy and the elastic energy, thus defining block copolymer melts with a different free energy. This can be contrasted with the difficulty to define, in an effective way, a homopolymer melt. One can keep a polymer at different temperatures for different times, but it is difficult to evaluate, quantitatively, the associated free energy. The second point regards strain-induced crystallization. The effect of external fields, such as shear and flow, etc, on the crystallization behavior, cannot be easily deduced from experiments. One difficulty is the nonuniform effect of external fields on the individual molecular chains. Both theory and experiments indicate that long chains may sustain a high stress,[34,35] which is assumed to be at the origin of the so-called shish kebab structures.[36,37] In ordered block copolymers, each crystallizable chain is connected with an amorphous one. This means that under stress the loss of entropy of each chain is about the same and can be evaluated. From this point of view, block copolymers are ideal model systems to investigate strain-induced crystallization.

CONCLUSIONS

The crystallization and melting behavior of short-chain symmetric diblock PEO-*b*-PB_h copolymers has been investigated with *in situ* SAXS. A continuous change of the long period was observed with increasing crystallization temperature, which indicates noninteger-folded chain crystals. A reorganization of the crystals has been deduced from the scattering intensity during slow heating. The confinement can be divided into the influence of diffusion and of nucleation. Crystallization experiments on samples cooled fast from different temperatures in the molten state reveal a significant coupling between the lamellar ordering and the crystallization. The reorganization of the chains during cooling promotes nucleation and shortens the induction period.

ACKNOWLEDGMENTS

The authors would like to thank Y. Séréro, R. Opitz, and I. Sikharulidze for valuable discussion. This work is part of the Softlink research program of the Stichting voor Fundamenteel Onderzoek der Materie (FOM), which is financially supported by the Nederlandse Organisatie voor Wetenschappelijk Onderzoek (NWO).

REFERENCES

1. Muthukumar, M.; Ober, C.K.; Thomas, E.L. Competing interactions and levels of ordering in self-organizing polymeric materials. Science **1997**, *277*, 1225.
2. DiMarzio, E.A. The ten classes of polymeric phase transitions: their use as models for self-assembly. Prog. in Polym. Sci. **1999**, *24*, 329.
3. Hong, S.; MacKnight, W.J.; Russell, T.P.; Gido, S.P. Structural evolution of multilayered, crystalline-amorphous diblock copolymer thin films. Macromolecules **2001**, *34*, 2876.

4. Zhu, L.; Chen, Y.; Zhang, A.; Calhoun, B.H.; Chun, M.; Quirk, R.P.; Cheng, S.Z.D.; Hsiao, B.S.; Yeh, F.J.; Hashimoto, T. Phase structures and morphologies determined by competitions among self-organization, crystallization, and vitrification in a disordered poly(ethylene oxide)-*b*-polystyrene diblock copolymer. Phys. Rev. B **1999**, *60*, 10022.
5. Wong, G.C.L.; Commandeur, J.; Fisher, H.; de Jeu, W.H. Orientational wetting in hybrid liquid crystalline block copolymers. Phys. Rev. Lett. **1996**, *77*, 5221.
6. Osuji, C.; Zhang, Y.; Mao, G.; Ober, C.K.; Thomas, E.L. Transverse cylindrical microdomain orientation in an LC diblock copolymer under oscillatory shear. Macromolecules **1999**, *32*, 7703.
7. Quiram, D.J.; Register, R.A.; Marchand, G.R.; Adamson, D.H. Chain orientation in block copolymers exhbiting cylindrically confined crystallization. Macromolecules **1998**, *31*, 4891.
8. Ryan, A.J.; Hamley, I.W.; Bras, W.; Bates, F.S. Structure development in semicrystalline diblock copolymers crystallizing from the ordered melt. Macromolecules **1995**, *28*, 3860.
9. Loo, Y.L.; Register, R.A.; Ryan, A.J. Modes of crystallization in block copolymer microdomains: breakout, templated, and confined. Macromolecules **2002**, *35*, 2365.
10. Kim, G.; Han, C.C.; Libera, M.; Jackson, C.L. Crystallization with melt ordered semicrystalline block copolymers: exploring the coexistence of microphase-separated and spherulitic morphologies. Macromolecules **2001**, *34*, 7336.
11. Chen, H.L.; Hsiao, C.; Lin, T.L.; Yamauchi, K.; Hasegawa, H.; Hashimoto, T. Microdomain-tailored crystallization kinetics of block copolymers. Macromolecules **2001**, *34*, 671.
12. Zhu, L.; Calhoun, B.H.; Ge, Q.; Quirk, R.P.; Cheng, S.Z.D. Crystal orientation changes in two-dimensionally confined nanocylinders in a poly(ethylene oxide)-*b*-polystyrene/polystyrene blend. Macromolecules **2001**, *34*, 6649.
13. Reiter, G.; Castelein, G.; Sommer, J.-U.; Rottele, A.; Thurn-Albrecht, T. Direct visualization of random crystallization and melting in arrays of nanometer-size polymer crystals. Phys. Rev. Lett. **2001**, *87*, 226101.
14. Bates, F.S.; Fredrickson, G. Dynamics of block copolymers: theory and experiment. Annu. Rev. Mater. Sci. **1996**, *26*, 501.
15. Helfand, E.; Wasserman, Z.R. Chapter 4. In *Developments in Block Copolymers I*; Applied Science Publishers: London, 1982; 99.
16. Richards, R.W. *Multicomponent Polymer Systems*; Wiley: New York, 1992; 103.
17. Hong, S.; MacKnight, W.J.; Russell, T.P.; Gido, S.P. Orientationally registered crystals in thin film crystalline/amorphous block copolymers. Macromolecules **2001**, *34*, 2398.
18. Hamley, I.W. *The Physics of Block Copolymers*; Oxford University Press: New York, 1998.
19. DiMarzio, E.A.; Guttmann, C.M.; Hoffman, J. Calculation of lamellar thickness in a diblock copolymer, one of whose components is crystalline. Macromolecules **1980**, *13*, 1194.
20. Whitmore, M.D.; Noolandi, J. Theory of crystallizable block copolymer blends. Macromolecules **1988**, *21*, 1482.
21. Vilgis, T.; Halperin, A. Aggregation of coil-crystalline block copolymers: equilibrium crystallization. Macromolecules **1991**, *24*, 2090.

22. Hong, S.; Yang, L.; MacKnight, W.J.; Gido, S.P. Morphology of a crystalline/amorphous diblock copolymer: poly((ethylene oxide)-*b*-butadiene). Macromolecules **2001**, *34*, 7009.
23. ten Wolde, P.R.; Frenkel, D. Enhancement of protein crystal nucleation by critical density fluctuations. Science **1997**, *277*, 1975.
24. Opitz, R.; Lambreva, D.M.; de Jeu, W.H. Confined crystallization of ethylene oxide-butadiene diblock copolymers in lamellar films. Macromolecules **2002**, *35*, 6930.
25. Wunderlich, B. *Macromolecular Physics*; Academic Press: New York, 1976; Vol. 2.
26. Hikosaka, M.; Keller, A.; Rastogi, S. Investigations on the crystallization of polyethylene under high pressure-role of mobile phases, lamellar thickening growth, phase-transformations, and morphology. J. Macromol. Sci. Phys. B **1992**, *31*, 87.
27. Turnbull, D. Kinetics of heterogeneous nucleation. J. Appl. Phys. **1950**, *21*, 1022.
28. Hoffman, J.D.; Weeks, J.J. Rate of spherulitic crystallization with chain folds in polychlorotrifluroethylene. J. Chem. Phys. **1962**, *37*, 1723.
29. Li, L.; Séréro, Y.; Koch, M.H.J.; de Jeu, W.H. Microphase separation and crystallization in an asymetric diblock copolymer: coupling and competition. Macromolecules **2003**, *36*, 529.
30. Cheng, C.Z.D.; Zhang, A.; Barley, J.S.; Chen, J.; Habenschuss, A.; Zschack, P.R. Isothermal thickening and thinning process in low-molecular-weight poly(ethylene oxide) fractions 1, from nonintegral-folding to integral-folding chain crystal transitions. Macromolecules **1991**, *24*, 3937.
31. Hu, W.; Albrecht, T.; Strobl, G. Reversible surface melting of PE and PEO crystallites indicated by TMDSC. Macromolecules **1999**, *32*, 7548.
32. Hikosaka, M. Unified theory of nucleation of folded-chain crystals (FCCS) and extended-chain crystals (ECCS) of linear-chain polymers. Polymer **1987**, *28*, 1257.
33. Hikosaka, M. Unified theory of nucleation of folded-chain crystals (FCCS) and extended-chain crystals (ECCS) of linear-chain polymers: 2. Origin of FCC and ECC. Polymer **1990**, *31*, 458.
34. Seki, M.; Thurman, D.W.; Oberhauser, J.P.; Kornfield, J.A. Shear-mediated crystallization of isotactic polypropylene: the role of long chain-long chain overlap. Macromolecules **2002**, *35*, 2583.
35. Bahar, I.; Erman, B.; Bokobza, L.; Monnerie, L. Molecular orientation in deformed bimodal networks. 1. Theory. Macromolecules **1995**, *28*, 225.
36. Somani, R.H.; Hsiao, B.S.; Nogales, A.; Srinivas, S.; Tsou, A.H.; Sics, I.; Balta-Calleja, F.J.; Ezquerra, T.A. Structure development during shear flow-induced crystallization of i-PP: in situ small-angle X-ray scattering study. Macromolecules **2000**, *33*, 9385.
37. Jerschow, P.; Janeschitz-Kriegl, H. The role of long molecules and nucleating agents in shear induced crystallization of isotactic polypropylenes. Int. Polym. Process. **1997**, *12*, 72.